Singlet Oxygen Trapping Porphyrins

A Major Qualifying Project Report:

submitted to the Faculty

of the

WORCESTER POLYTECHNIC INSTITUTE

in partial fulfillment of the requirements for the

Degree of Bachelor of Science in Chemistry

By

Daniel W. Carney

Date: January 8, 2009

Approved:

Professor Robert E. Connors, Advisor

Abstract

Chemical and biological attacks pose a very concerning threat to armed service personnel and national security in general. One of the leading responses to this threat has been the development of "Self-detoxifying materials." There is currently a great deal of interest in the development of singlet oxygen sensitizing and trapping systems as self-detoxifying materials. This report documents the synthesis and preliminary testing of a novel singlet oxygen sensitizing and storing molecule. Pyridone linked zinc tetraphenylporphine has been synthesized via a Lindsey type pathway. Using H-NMR, it has been demonstrated that both pyridone linked zinc tetraphenylporphine as well as the free base pyridone linked tetraphenylporphine have the ability to reversibly sensitize and store singlet oxygen in the form of an endoperoxide repeatedly without being decomposed.

Acknowledgements

I would like to sincerely thank Dr. Chuchawin Changtong for his advice regarding porphyrin synthesis as well as Professor Robert E. Connors for his guidance and assistance throughout the project. Also, I would like to thank Professor Venkat R. Thalladi, Professor James W. Pavlik, and Christopher Zoto for their support and advice. Finally I would like to thank Dr. Heidi Schreuder-Gibson and the U.S. Army Natick Soldier Research, Development & Engineering Center for helping to make this project possible.

Table of Contents

Abstract ii
Acknowledgements iii
List of Figures v
List of Tables v
Introduction 1
Background 3
  Singlet Oxygen 3
  Porphyrins 5
  Endoperoxides 8
Experimental 10
  Synthesis of P-(a-bromo)methyl Benzaldehyde 10
  Synthesis of the Tetrakis (a-bromo-p-tolyl)porphyrin 16
  Synthesis of Pyridone Linked Tetraphenylporphine 20
  Synthesis of the Pyridone Linked Zinc Tetraphenylporphine 22
  Effects of Metallation on Absorbance Properties 23
  Irradiation of Pyridone Linked Porphyrins 24
Results 26
  UV/Vis absorbance properties 26
  Reversible Endoperoxide Formation 27
Discussion 31
References 33

List of Figures

Figure 1 - Structure of Porphine 6
Figure 2 - General Reaction for Porphyrin Synthesis 7
Figure 3 - Reversible [1+2] Cycloaddition of Singlet Oxygen to N-Substituted Pyridone .8
Figure 4 - Structure of 2-Pyridone Linked Zinc Tetraphenylporphine 9
Figure 5 - H-NMR Spectrum of the Crude P-Bromomethyl Benzaldehyde Product in $CDCl_3$ 12
Figure 6 - H-NMR Spectrum of the Crude P-Bromomethyl Benzaldehyde Product Blown up Between 4.34 and 4.44 ppm 13
Figure 7 - H-NMR Spectrum of Column Chromatography Purified P-Bromomethyl Benzaldehyde in $CDCl_3$ 14
Figure 8 - H-NMR Spectrum of Column Chromatography Purified P-Bromomethyl Benzaldehyde Blown up Between 4.1 and 4.7 ppm 15
Figure 9 - H-NMR Spectrum of Tetrakis (a-bromo-p-tolyl)porphyrin in $CDCl_3$ 18
Figure 10 - NMR Spectrum of Pyridone Linked Tetraphenylporphine in DMSO-d6 21
Figure 11 - H NMR Spectrum of Pyridone Linked Zinc Tetraphenylporphine in DMSO-d6 23
Figure 12 - UV/VIS Spectra of Metallated and Free Base Pyridone Linked Porphyrins ..26
Figure 13 - UV/VIS Spectra of Metallated and Free Base Pyridone Linked Porphyrins Expanded in Q Band Region 27
Figure 14 - Endoperoxide Formation Reaction 27
Figure 15 - Overlay of H-NMR Spectra in $CDCl_3$ from Free Base Pyridone Linked TPP Irradiation Experiment 28
Figure 16 - Overlay of H-NMR Spectra in DMF-d7 from Pyridone Linked ZnTPP Irradiation Experiment 29

List of Tables

Table 1 - Irradiation and Heating Cycles of Free Base Pyridone Linked TPP 25
Table 2 - Irradiation and Heating Cycles of Pyridone Linked Zinc TPP 25

Introduction

Chemical and biological attacks pose a very concerning threat to armed service personnel and national security in general. Such weaponry has in recent history become prevalent in terrorist attacks as well as international conflicts despite being condemned by the Geneva Protocol and more recently the 1972 Biological and Toxin Weapons Convention.[1] A developing approach to individual protection from chemical and biological attack incorporates the use of "self-detoxifying materials." Self-detoxifying materials include polymers and surface coatings that are able to react with harmful chemical and biological agents.

Ideally, these reactive materials should be effective against a wide range of chemical and biological agents and should be self-regenerating. Singlet oxygen generating and trapping molecules are of particular interest because singlet state oxygen is known for its powerful oxidizing ability. Many different chemical and biological agents are subject to detoxification by oxidation.[2] Additionally, neither the sensitizing nor the storing components are used up in their reactions to form and reversibly trap singlet oxygen. A well functioning singlet oxygen generating and storage material should be able to generate singlet state oxygen from triplet state oxygen in the atmosphere and reversibly store it so that it may be released when needed. After singlet oxygen is released from the storage component, the same material should then be able to proceed through the singlet oxygen generation and trapping process again.

The concept of composite molecules which generate, store, and release singlet oxygen is derived from the work of Dr. Chuchawin Changtong et al.[3] Changtong was the first to synthesize free base pyridone linked tetraphenylporphine. The goal of this project

was to synthesize pyridone linked zinc tetraphenylporphine as well as to improve upon Dr. Changtong's established synthetic procedure. Porphyrins are known to have the ability to photosensitize singlet oxygen and 2-pyridone is known to have the ability to reversibly store singlet oxygen in the form of endoperoxides.[4-5] The compound that has been synthesized in this project contains a porphyrin backbone and four pyridine groups in a single molecule. This report contains in detail, the procedure used to synthesize the desired compound as well as the results of an NMR study, which demonstrates the reversible formation of endoperoxides by the free base pyridone linked TPP and the pyridone linked ZnTPP.

Throughout the report, the terms tetraphenylporphine and TPP will be used interchangeably. Additionally, the suffix "porphine" is used in the naming of compounds that are classified as porphyrins. Nevertheless, it is common to find the suffixes "porphine" and "porphyrin" used interchangeably throughout the literature.

Background

Singlet Oxygen

The ground state molecular form of oxygen, which is abundant in the air we breathe every day, contains two unpaired valence electrons. The molecular orbital electron configuration is as follows:

$$O_2 \rightarrow (\text{core})(\pi_x\uparrow\downarrow)(\pi_y\uparrow\downarrow)(\pi_x{*}\uparrow)(\pi_y{*}\uparrow)$$

However, only the two anti-bonding π electrons are important for describing singlet state oxygen. If all but the two highest energy electrons are ignored, the electron configuration is as follows:[6]

$$O_2 \rightarrow (\pi_x{*}\uparrow)(\pi_y{*}\uparrow)$$

In the ground state of molecular oxygen the two highest energy electrons have spins aligned in the same direction. This electronic configuration is known as a triplet state and is given the notation $^3\Sigma$. In addition to its ground triplet state, molecular oxygen also has two low energy excited singlet states. In these two excited states, the two highest energy electrons have opposite spins and can either be paired or unpaired. The notations for the paired and unpaired electron configurations are $^1\Delta$ and $^1\Sigma$ respectively. The electronic configurations are as follow:

$^1\Delta O_2 \rightarrow (\pi_x^*\uparrow\downarrow)$ or $(\pi_y^*\uparrow\downarrow)$

$^1\Sigma O_2 \rightarrow (\pi_x^*\uparrow)(\pi_y^*\downarrow)$

It is important to note that $^1\Delta O_2$ can have its highest energy electrons in either the π_x^* or the π_y^* orbitals. Because these two orbitals are degenerate, there is no distinction between the two in the context of this study. It is also important to note that $^1\Delta O_2$ is lower in energy than $^1\Sigma\ O_2$.[6] Although both states can be referred to as 'singlet oxygen,' for the purpose of this report, the term 'singlet oxygen' will refer only to $^1\Delta O_2$.

The chemistry and physical properties of singlet oxygen have been studied intensely since 1965, when Khan and Kasha interpreted the chemiluminescence of the hypochlorite-peroxide reaction caused by liberated singlet oxygen.[4] Chemiluminesence is a chemical phenomenon which occurs when a portion of the free energy (ΔG) of a reaction is converted to electronic excitation. Singlet oxygen can be generated and often times react via chemiluminescent pathways.[6] The reason why Singlet oxygen is of particular interest in this study is because it is a very strong oxidizing reagent. Singlet oxygen is known to be both biocidal and have the ability to react with a variety of chemical warfare agents that are susceptible to oxidation. Another important property of singlet oxygen is its long lifetime which is a result of the fact that direct transition from $^1\Delta O_2 \rightarrow {}^3\Sigma O_2$ is spin forbidden.[4]

There are many different methods for generating singlet oxygen. Although direct photoexcitation is possible, it is most commonly generated via energy transfer from a photosensitizer. Singlet oxygen is generated by a photosensitizer via the following mechanism. First the photosentitizer must be excited to the first excited singlet state

($S_0 \rightarrow S_1$). Then the excited state must undergo intersystem crossing to the first excited triplet state ($S_1 \rightarrow T_1$). Ground state triplet oxygen can then undergo an energy transfer with the photosensitizer upon collision to produce singlet oxygen and the photosensitizer in its ground singlet state.[4]

It is also known that singlet oxygen can be produced from the thermal decomposition of certain endoperoxides, a chemiluminescent process.[6] This study implements both of these forms of singlet oxygen generation. The final molecule utilizes porphyrins as a photosensitizer and 2-pyridone as an endoperoxide precursor, both of which are discussed in the subsequent background sections.

Porphyrins

Porphyrins are a class of heterocyclic macrocycles known for their intense colors. Porphyrins and closely related compounds are found commonly throughout nature. The word porphyin comes from the Greek word for purple, as all porpyrins have very vibrant colors, many of which are purple.[7] The porphyrin ring consists of four pyrrole subunits linked together by methine bridges. Each atom in the macrocycle is sp2 hybridized, making the ring completely conjugated with 22 π electrons but only 18 completely delocalized.[2]

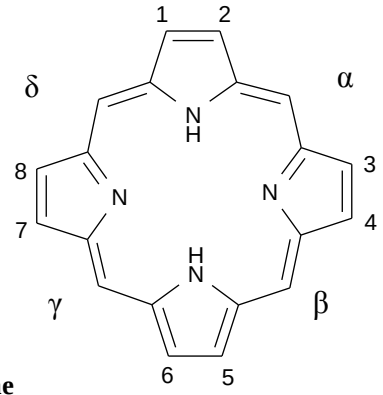

Figure 1 - Structure of Porphine

Figure 1 shows the chemical structure of porphine, which is the simplest porphyrin and the backbone upon which all porphyrins are derived.[2] The numerals and Greek letters denote the many possible sites for substituents.

The porphyrin ring is aromatic, as it is planar and obeys Huckel's Rule. Consequently, it is also very stable. Porphyrins which contain carboxylic acid side chains usually do not have a melting point, and esters and metal complexes sometimes melt between 200-300˚C often without decomposing.[2]

A second consequence of a porphyrins' high degree of conjugation is its characteristic electronic absorption spectrum. The visible light spectrum of a typical porphyrin contains a very intense absorption around 400 nm known as the Soret band, which represents the $S_0 \rightarrow S_2$ transition, and several absorptions between 500 and 650 nm known as the Q band, which represents the $S_0 \rightarrow S_1$ transition. The Q band consists of multiple peaks corresponding to different vibrational modes. The second excited singlet state can decay to the first excited singlet state and from there undergo intersystem crossing to the first excited triplet state.[2] The long-lived triplet state and high triplet quantum yield of most porphyrins make them efficient singlet oxygen photosensitizers. Furthermore, typical porphyrin absorption bands overlap with important components of sunlight, which suggests that if the target molecule of this synthesis were to be

incorporated into a fabric system, self-detoxifying properties could be established simply from exposure to direct sunlight.[4]

There are an infinite number of molecules that can be derived from the basic porphyrin backbone, porphine. The class of porphyrins that this study is interested in are known as *meso*-substituted porphyrins, where substitituents are located at the α,β,γ, and δ positions.[2] *Meso*-substituted porphyrins in which all four substiuents are the same can be synthesized in the laboratory via the general reaction shown below discovered by Paul Rothemund in 1935.[8-9]

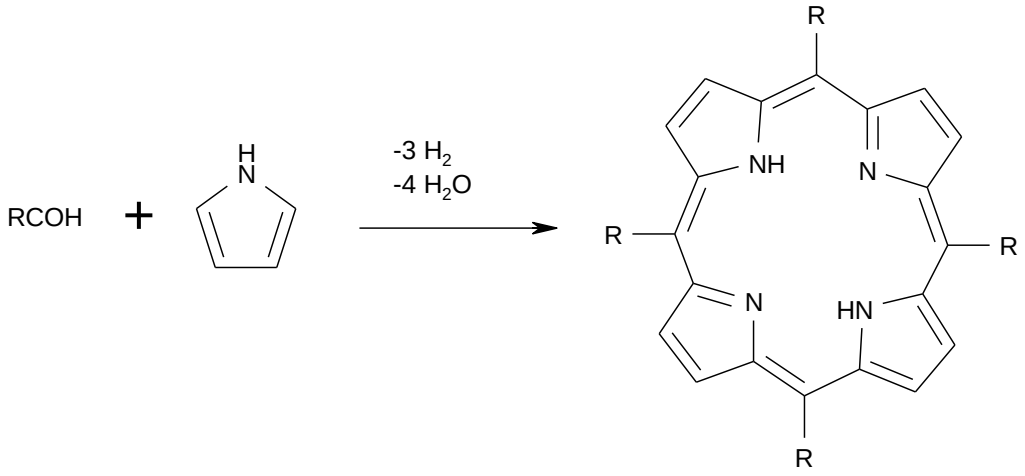

Figure 2 - General Reaction for Porphyrin Synthesis

The reaction is carried out in one pot with two steps. First pyrrole and an aldehyde are combined in the presence of an acid catalyst followed later by an oxidizing reagent such as dichloro dicyano quinone (DDQ). Although many reaction pathways have been discovered for producing *meso*-substituted porphyrins, this method, developed by Jonathan Lindsey et al, is preferred because the mild conditions are compatible with many sensitive aldehydes.[10]

Endoperoxides

Singlet oxygen reacts with 1,3-diene systems in a [4+2] cycloaddition reaction to form an important class of compounds known as endoperixides. Endoperoxides are molecules witch contain a peroxide bridge (-O-O-) between two atoms which are both part of a larger molecule. They are synthetically very useful, able to undergo a wide variety of transformations to form diols, carbonyl compounds, epoxides, and furan derivatives just to name a few.[11] What is of particular interest to this study however, is the ability of some endoperoxides to release singlet oxygen upon thermalization.

It is known that that singlet oxygen can undergo [4+2] cycloaddition with N-substituted Pyridones to yield 1,4-endoperoxides. Furthermore, the endoperoxides can decompose to yield the corresponding pyridones while liberating singlet oxygen in high yield.[5]

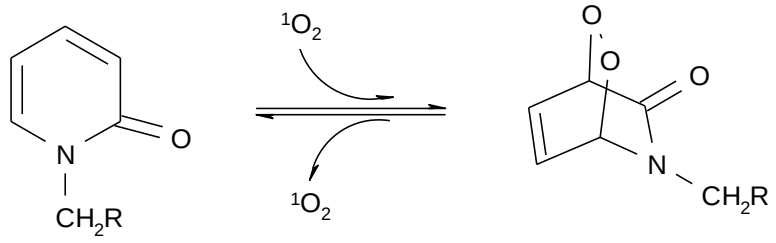

Figure 3 - Reversible [1+2] Cycloaddition of Singlet Oxygen to N-Substituted Pyridone

Masakatsu Matsumoto[5] has reported that in the reaction schematic shown in figure 3, reversible endoperoxide formation will take place when 'R' is a phenyl group. It is known that tetraphenylporphine (TPP) is a good sensitizer of singlet oxygen.[5,11] Furterhmore, it is known that coordinating a zinc ion to the center of TPP increases the quantum yield of the triplet state.[4] These facts are the foundation for the hypothesis that

2-pyridone linked zinc tetraphenylporphine is a highly efficient singlet oxygen sensitizing and trapping molecule.

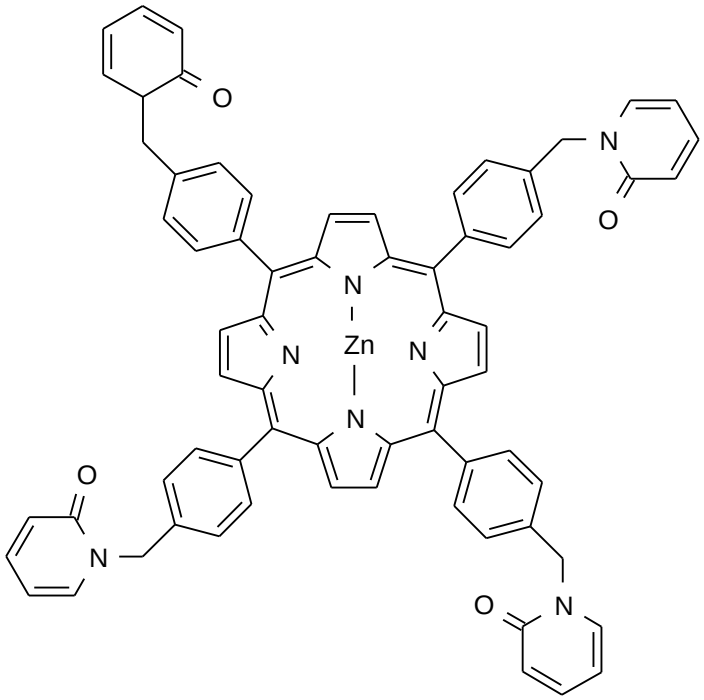

Figure 4 - Structure of 2-Pyridone Linked Zinc Tetraphenylporphine

Experimental

Synthesis of P-(a-bromo)methyl Benzaldehyde

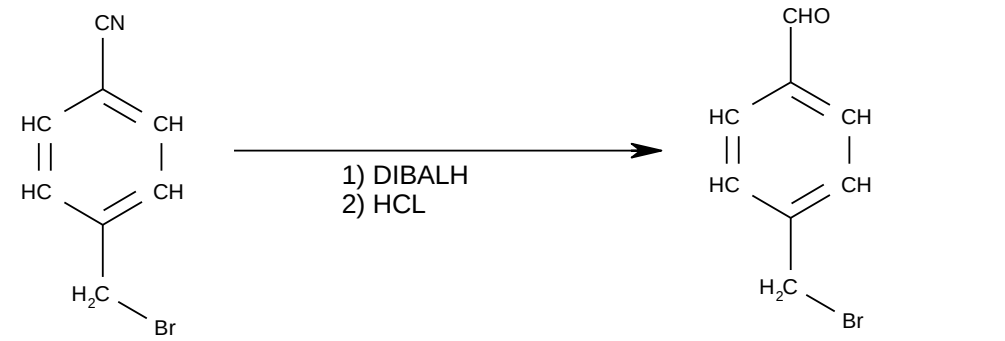

Molecular Weight =196.05
Exact Mass =196
Molecular Formula =C8H6BrN
Molecular Composition =C 49.01%
H 3.08% Br 40.76% N 7.14%

Molecular Weight =199.05
Exact Mass =199
Molecular Formula =C8H7BrO
Molecular Composition =C 48.27%
H 3.54% Br 40.14% O 8.04%

Before the actual porphyrin can be synthesized, an aldehyde precursor must be generated. This transformation is carried out via reduction of a nitrile using diisobutylaluminum hydride (DIBALH,) followed by acid catalyzed hydrolysis.

In a typical reaction, a dropping funnel and a three neck round bottom flask containing a magnetic stirring bar were stored in an oven set to 110 C over night. Upon removal from the oven, α-bromo-p-tolunitrile (1.00-3.00 g) was immediately added to the round bottom flask. The dropping funnel was then fixed to the round bottom flask and all open ends were sealed with rubber septa. A number of steps were then taken to ensure that the system was completely anhydrous. First, dry argon was passed through the system for 30 minutes. Secondly, the system was blow dried under vacuum for approximately 15 minutes.

With anhydrous conditions established, toluene (anhydrous) was added to the flask via solvent bridge through the septum. A solvent bridge was constructed using a double headed syringe needle, which served as a link between the sealed solvent bottle and the sealed reaction flask. Dry argon was fed into the solvent bottle to provide back pressure thus forcing the solvent through the bridge. A balloon fastened to a syringe needle was used to relieve the excess pressure generated in the reaction flask as a result of the solvent addition. Solvent was added until the flask was roughly half full. The contents of the flask were then stirred until all of the a-bromo-p-tolunitrile was dissolved.

Once the solution was homogeneous, the reaction flask was suspended in a thermal control bath set to 0˚C for 30 minutes before the addition of the second reactant. DIBALH (1M solution in toluene) was added to the dropping funnel via solvent bridge in a similar manner as the toluene. The mole ratio of DIBALH to nitrile varied from 1.3:1 to 1.5:1. Too much DIBALH can lead to the reduction of the nitrile to a primary amine. However, a slight excess is used because the DIBALH can be spontaneously oxidized by any residual water in the system. Very slight bubbling was commonly observed in the DIBALH solution upon addition to the dropping funnel. The DIBALH was slowly added to the cold reaction solution and allowed to react for 2 hours at low temperature. The reaction flask was removed from the thermal control bath and then allowed to react with stirring at room temperature for an additional 3 hours. Over the course of the reaction, the solution turned from completely clear to light yellow.

With the DIBALH given plenty of time to react, one of the septa was removed from the reaction flask and a solution of HCl (.06M in water) was added to the solution. The volume of HCl solution used was approximately 2/3 the volume of organic solvent

already in the flask. Almost immediately, a white precipitate began to form and the solution became clear. The reaction was allowed to proceed with stirring for an hour.

After the reaction, the solution was filtered. Most of the white solid remained inside the reaction flask. It had a paste like consistency and was very sticky. Dichloromethane was added to the filtrate and the organic phase was separated from the aqueous phase. The aqueous phase was washed three times with 50mL of dichloromethane, each time collecting the organic phase. The organic solution was dried with anhydrous sodium sulfate over night. The dried solution was gravity filtered and then concentrated leaving behind a white/yellow solid. The solid was analyzed by TLC (80% dichloromethane, 20% hexanes) and proton NMR. TLC revealed that the solid was a mixture of two or more components with spots at Rf=0.6 and Rf=0.67.

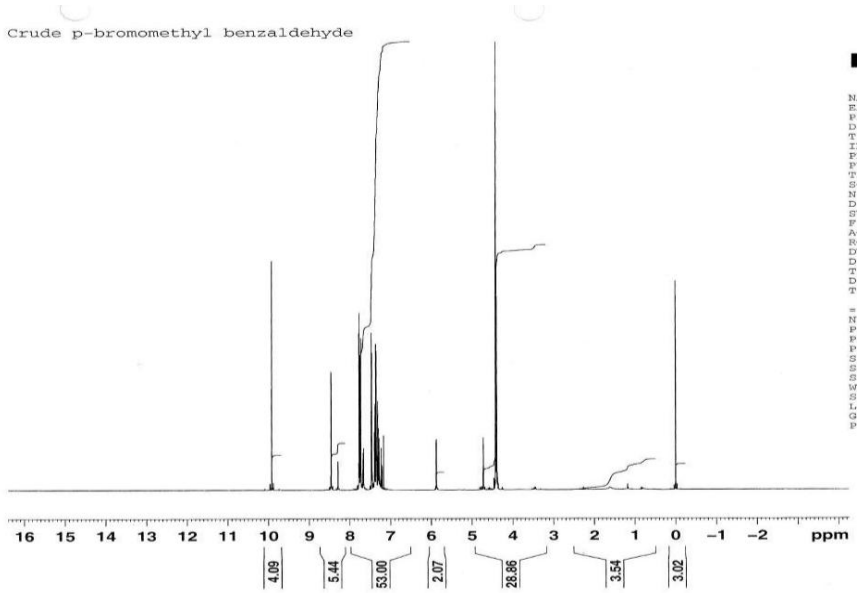

Figure 5 - H-NMR Spectrum of the Crude P-Bromomethyl Benzaldehyde Product in $CDCl_3$

Shown in figure 5 is the proton NMR spectrum of crude p-bromomethyl benzaldehyde in deuterated chloroform. The singlet at 9.9 ppm is characteristic of an aldehyde. Signals representing the ortho and meta protons of the benzene ring appear in the region between

7 and 8 ppm. Several singlet's of varying intensities appear around 4.4 ppm and are representative of the various CH2Br protons present in the various components in the crude solid.

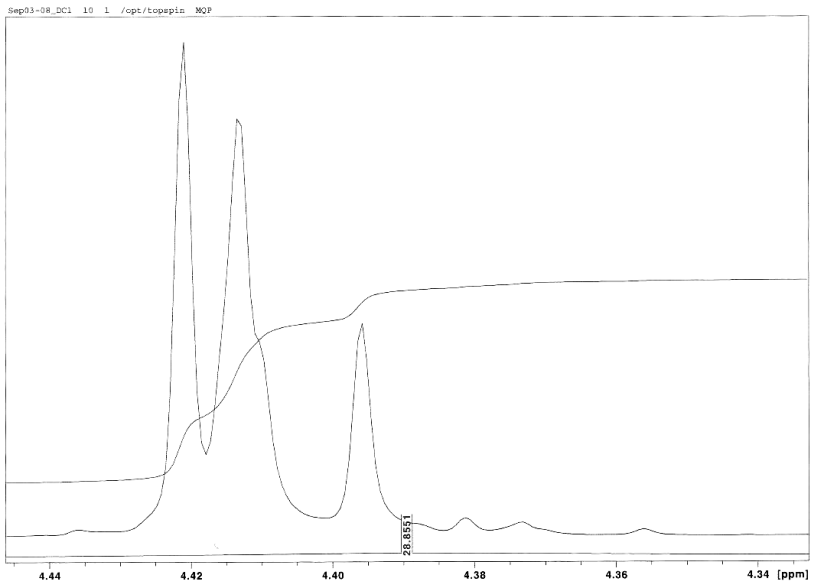

Figure 6 - H-NMR Spectrum of the Crude P-Bromomethyl Benzaldehyde Product Blown up Between 4.34 and 4.44 ppm

Shown in figure 6 is the H-NMR spectrum of crude p-bromomethyl benzaldehyde blown up between 4.34 and 4.44 ppm. The 3 singlets represent the CH_2Br protons of p-bromomethyl benzaldehyde (4.42 ppm) as well as the nitrile starting product (4.41 ppm) and p-bromomethyl benzamine side product (4.395 ppm).

P-bromomethyl benzaldehyde was successfully purified via column chromatography. Silica gel was used as a stationary phase and mixtures of hexanes and dichloromethane were used as the eluting solvent. The pure product was eluted very carefully from the column. A solvent gradient was used beginning first with pure hexanes followed by a 10% increase in dichloromethane with each subsequent 150mL of

eluting solvent used. The product was collected in 16 mL (4 dram) fractions and analyzed by TLC (80% dichloromethane, 20% hexanes). TLC revealed that the first 8 fractions contained p-bromomethyl benzaldehyde and impurities. All subsequent fractions contained only the desired product. Proton NMR analysis also revealed that p-bromomethyl benzaldehyde was isolated in high purity. The gradual increase in solvent polarity was extremely important. Several column's were run without a gradient as well as with changes in polarity that were not as gradual as described, all of which resulted in incomplete separation of the benzaldehyde from the benzonitrile.

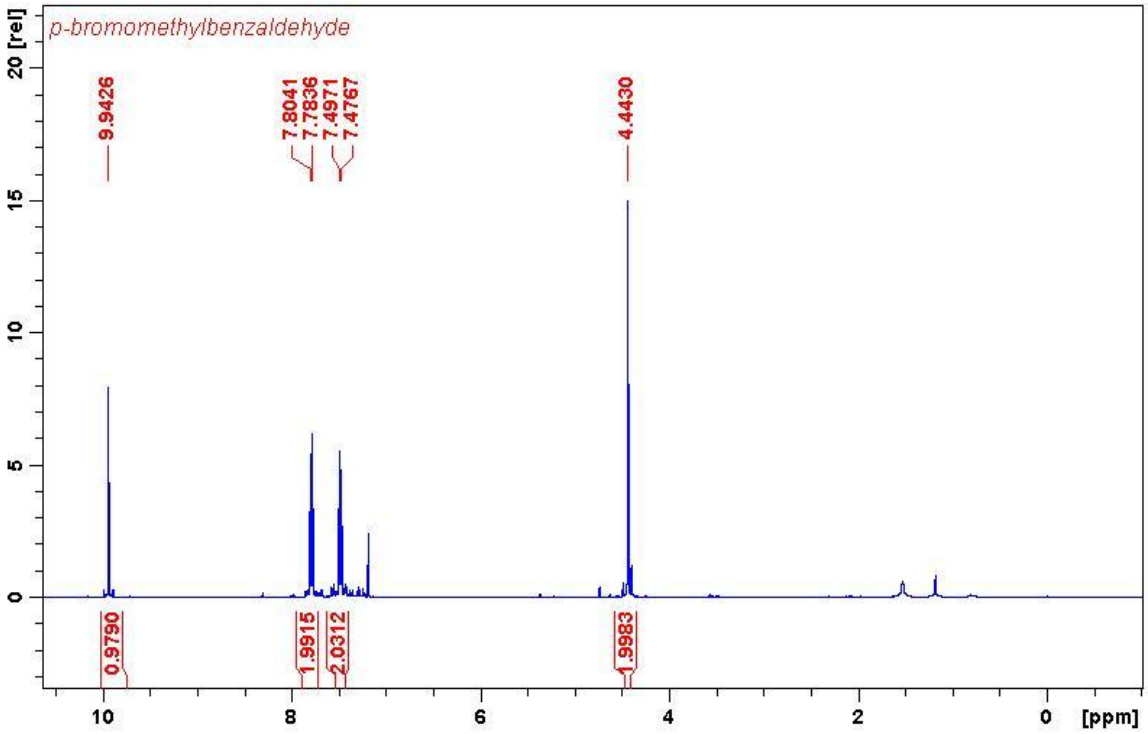

Figure 7 - H-NMR Spectrum of Column Chromatography Purified P-Bromomethyl Benzaldehyde in $CDCl_3$

Shown in figure 7 is the proton NMR spectrum of p-bromomethyl benzaldehyde after purification via column chromatography. The singlet at 4.5 ppm corresponds to the

CH_2Br protons. The meta and ortho protons correspond to the signals at 7.4 ppm and 7.8 ppm respectively. The aldehyde proton is represented by the singlet at 9.9 ppm.

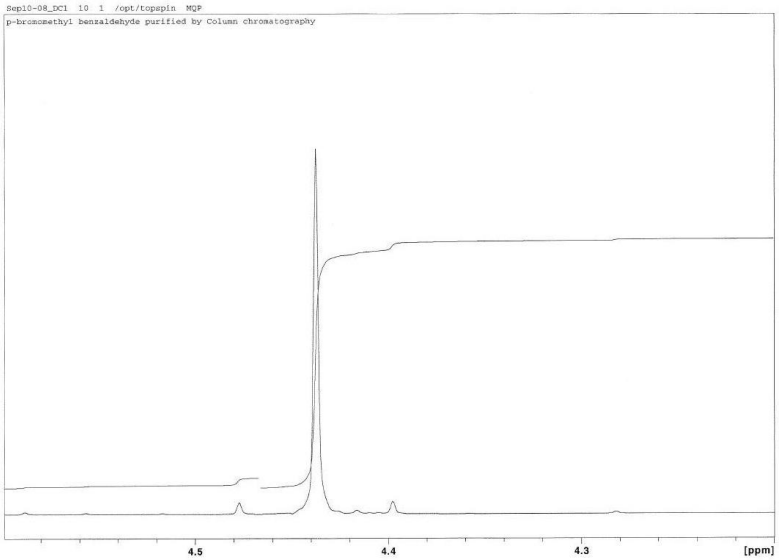

Figure 8 - H-NMR Spectrum of Column Chromatography Purified P-Bromomethyl Benzaldehyde Blown up Between 4.1 and 4.7 ppm

Shown in figure 8 is the proton NMR spectrum of purified p-bromomethyl benzaldehyde blown up between 4.1 and 4.7 ppm. This portion of the spectrum shows the singlet that represents the CH_2Br protons of p-bromomethyl benzaldehyde. The side bands at 4.39 ppm and 4.48 ppm are a result of poor shimming on the NMR spectrometer. The absence of other signals in this region shows that the solid product no longer contains significant amounts of nitrile or amine.

As an alternative to column chromatography, the aldehyde can also be purified via adduct formation with sodium bisulfite. In this procedure, a crude solution of p-bromomethyl benzaldehyde in toluene/dichloromethane was stirred with a saturated sodium bisulfite solution in a 70:30 mixture of ethanol and water. The aqueous phase

was isolated and acidified with concentrated hydrochloric acid. Upon the addition of hydrochloric acid, the aqueous solution was added to anhydrous ether and stirred. The aqueous solution was washed with ether (50mL) a total of four times. The ether was collected and dried over anhydrous sodium sulfate. Finally the ether was filtered and evaporated leaving behind pure p-bromomethyl benzaldehyde. Ultimately, the purification procedure was successful; however the yield was very low.

In order to conserve time, the p-bromomethyl benzaldehyde may be used in subsequent reactions without being fully purified. Typically the crude solution was concentrated to only a few mL then subjected to a silica column with 3" bed height. The toluene was first eluted with 100% hexanes, followed by 100% dichloromethane to elute the product. The product containing solution was then air dried in a pyrex bowl leaving solid white and yellow colored crystals confirmed by H-NMR to be p-bromomethyl benzaldehyde (>80% pure.)

Synthesis of the Tetrakis (a-bromo-p-tolyl)porphyrin

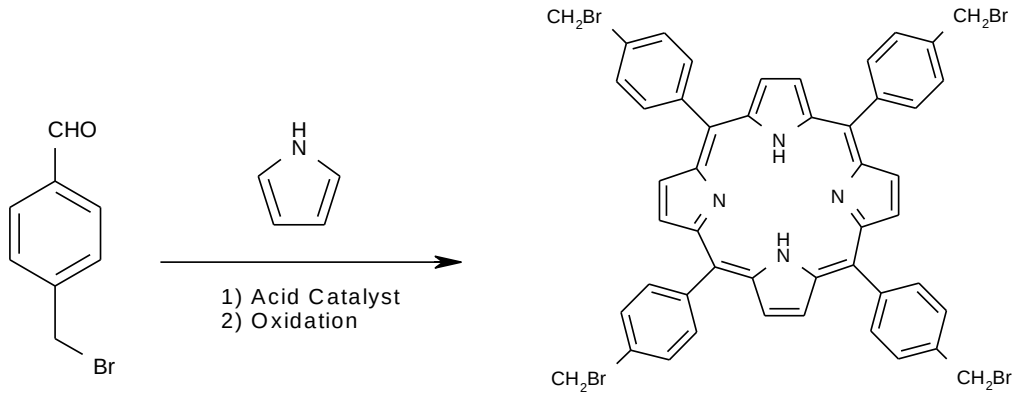

Molecular Weight =199.05
Exact Mass =199
Molecular Formula =C8H7BrO
Molecular Composition =C 48.27% H 3.54% Br 40.14% O 8.04%

Molecular Weight =670.86
Exact Mass =670
Molecular Formula =C48H38N4
Molecular Composition =C 85.94% H 5.71% N 8.35%

Similar to the aldehyde precursor, the tetrakis (a-bromo-p-tolyl)porphyrin was synthesized under anhydrous conditions. The reactor used was a single 500 mL round bottom flask with a magnetic stirring bar. The round bottom flask was stored with a magnetic stir bar at 110˚C over night. First, the aldehyde and amberlyst ion exchange resin (4.00g constant) were added to the empty flask. With the two solid reactants added to the flask, the three open ends were sealed with rubber septa.

To establish anhydrous conditions, the flask was filled with argon and then blow dried under vacuum. Anhydrous chloroform was then added to the flask via solvent bridge through one of the septa until the flask was about 2/3 full. A balloon was attached to a syringe needle which penetrated a second septum in order to relieve excess pressure inside the flask. The contents of the flask were stirred until all of the aldehyde was dissolved. Finally, to ensure anhydrous conditions, the system was flushed with dry argon for 15 minutes.

Before adding any more reactants, the round bottom flask was wrapped in aluminum foil to shield the solution from ambient light. Pyrrole was added to the aldehyde solution via syringe through the septum and stirred for 5 hours. The mole ratio of pyrole to aldehyde was always 1:1. Over the course of the reacting period the solution changed from colorless to dark red. Color change was clearly noticeable after about 30 minutes. After the 5 hours, a septum was removed, and dichlorodicyanno quinone (DDQ) was added to the flask. The DDQ was always added in a 1:1 mole ratio to the aldehyde starting material. The solution quickly turned very dark and opaque. After 40 minutes, the entire contents of the reaction solution were filtered through a column of neutral alumina with a bed height of approximately 3 inches. A red/purple solution was

eluted from the column. Excess dichloromethane was added to the column until the eluting solvent had no color.

The entire eluted solution was concentrated to a shiny purple solid. The solid was analyzed by TLC (100 % dichloromethane) and H-NMR in $CDCl_3$. TLC analysis revealed that the solid contained only one component characterized by a spot with Rf = 0.9, which fluoresced bright orange under a UV lamp set on long wavelength. H-NMR of the solid revealed that it was tetrakis(a-bromo-p-tolyl)porphyrin.

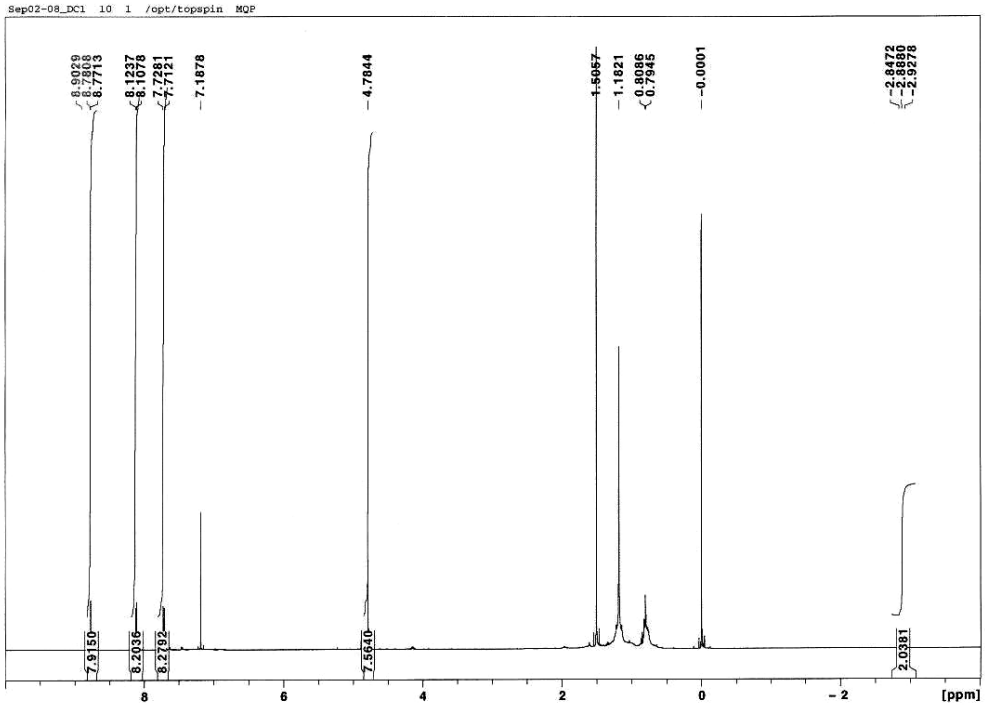

Figure 9 - H-NMR Spectrum of Tetrakis (a-bromo-p-tolyl)porphyrin in $CDCl_3$

Shown in Figure 9 is the proton NMR spectrum of Tetrakis (a-bromo-p-tolyl)porphyrin. The 2 proton singlet at -2.8 ppm is characteristic of the protons in the inner core of the porphyrin. The 8 proton singlet at 4.8 ppm represents the CH_2Br protons. The ortho and meta phenyl protons give rise to 8 proton signals at 7.8 ppm and 8.2 ppm respectively.

The downfield 8 proton singlet at 8.86 ppm corresponds to the pyrrolic protons on the porphyrin ring. The remaining signals are due to solvent impurities.

In the early stages of the project a different workup procedure was used to isolate tetrakis(a-bromo-p-tolyl)porphyrin. First, triethylamine (TEA) was added to gravity filtered crude reaction solution. A small amount of solution was then removed from the round bottom flask and diluted with dichloromethane to observe the color. Often times the solution turned green, a consequence of the porphyrin coordinating two extra protons to its inner core in acidic media. TEA was added to the solution until diluted aliquots of the crude solution appeared purple or pink. Once the free base porphyrin was obtained, the crude solution was concentrated and developed on a silica gel column to obtain purified tetrakis(a-bromo-p-tolyl)porphyrin. This workup procedure is not recommended however, because it prolongs the exposure of the porphyrin to excess DDQ, which can cause it to decompose over time. Several reactions were attempted using the aforementioned workup procedure that resulted in no recovery of the desired porphyrin product.

Synthesis of Pyridone Linked Tetraphenylporphine

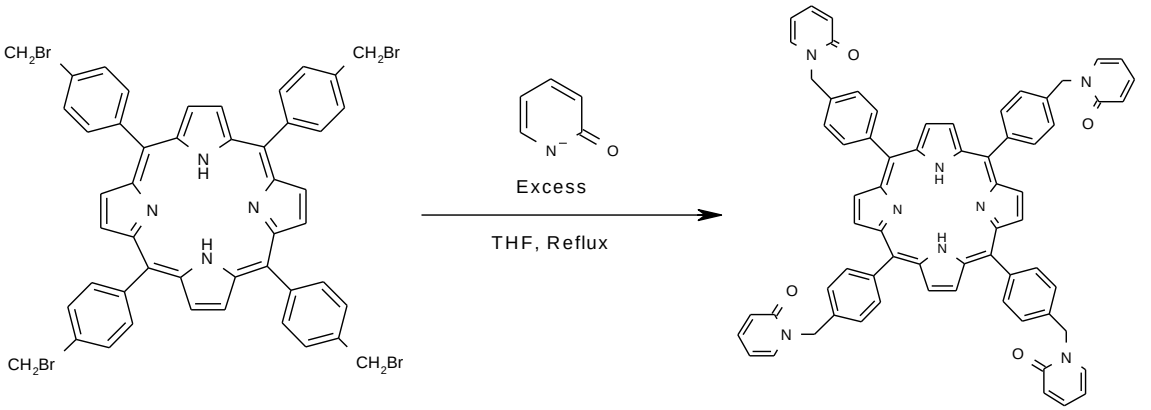

Molecular Weight =670.86
Exact Mass =670
Molecular Formula =C48H38N4
Molecular Composition =C 85.94% H 5.71% N 8.35%

Molecular Weight =1043.21
Exact Mass =1042
Molecular Formula =C68H50N8O4
Molecular Composition =C 78.29% H 4.83% N 10.74% O 6.13%

The third step of the synthesis was yet another anhydrous reaction. 2-hydroxy pyridine and the tetrakis (a-bromo-p-tolyl)porphyrin were weighed in separate 50 mL round bottom flasks. The mole ratio of 2-hydroxy pyridine to porphyrin was 8:1. The two flasks were sealed with rubber septa and purged with argon for ~15 minutes each. A 50 mL round bottom flask containing a magnetic stir bar and a cold water condenser were stored at 110˚C over night. Sodium hydride was added to the round bottom flask immediately after its removal from the oven. The mole ratio of sodium hydride to porphyrin was also 8:1. Once the sodium hydride was added to the reaction flask, the condenser was attached and the apparatus was sealed with a septum. The sealed apparatus was purged with argon and then flame dried under vacuum.

With anhydrous conditions established, THF (10 mL) was added to the flask containing 2-hydroxypyridine to dissolve the solid. The solution was then transferred into the reaction flask via solvent bridge. The solution bubbled for about a minute after the addition of the 2-hydroxy pyridine to the sodium hydride. The contents were stirred for an hour at which point the tetrakis (a-bromo-p-tolyl)porphyrin was added to the

reaction flask in the same manner as the 2-hydroxy pyridine. The purple solution was refluxed for four hours.

At the end of the reaction, there was a red/purple precipitate in the flask and the color of the solution was a light purple color. The solid precipitate was filtered then washed with dichloromethane. Dichloromethane dissolved most of the solid and generated a dark red/purple filtrate. A yellow/brown solid was left behind on the filter paper. The filtrate was concentrated to a red/purple solid. The solid was analyzed by H-NMR in DMSO-d6 and confirmed to be pyridone linked tetraphenylporphine.

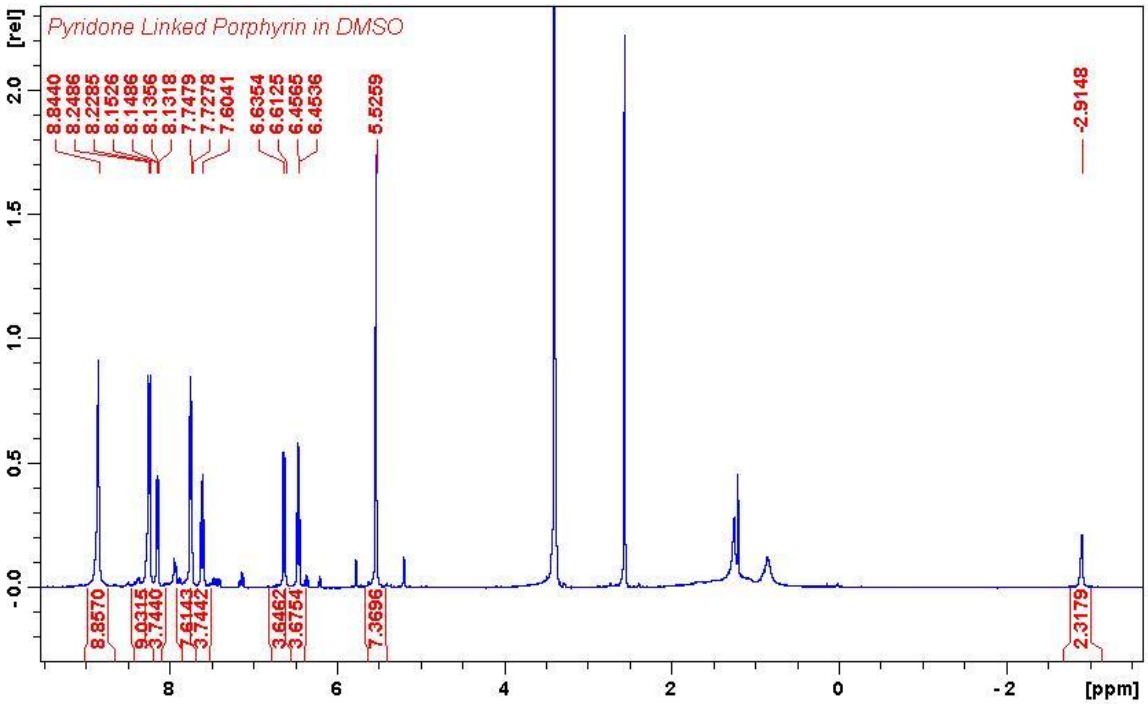

Figure 10 - NMR Spectrum of Pyridone Linked Tetraphenylporphine in DMSO-d6

Shown in figure 10 is the proton NMR spectrum of pyridone linked TPP. The 2 proton singlet at -2.9ppm represents the two hydrogens in the porphyrin inner core. At 5.5 ppm there is an 8 proton singlet which represents the methylene hydrogens in the porphyrin-pyridone link. The pyridone hydrogens give rise to a 4 proton triplet at 6.4 ppm, a 4

proton doublet at 6.6 ppm, a 4 proton triplet at 7.6 ppm and a 4 proton doublet at 8.1 ppm. The ortho and meta phenyl hydrogens give rise to doublets at 7.8 ppm and 8.2 ppm. The pyrrolic hydrogens on the porphyrin ring give rise to an 8 proton singlet at 8.8 ppm. The peaks between 0 ppm and 4 ppm are all solvent impurities.

Synthesis of the Pyridone Linked Zinc Tetraphenylporphine

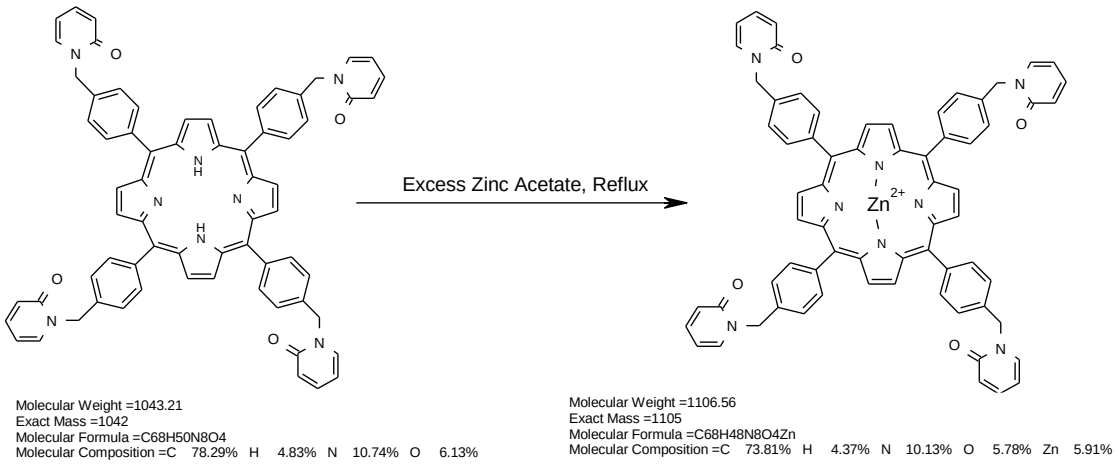

Zinc Acetate was added to a 100 mL round bottom flask with methanol (~10 mL) and stirred until completely dissolved. The pyridone linked tetraphenylporphine was dissolved separately in dichloromethane. The porphyrin solution was added to the zinc acetate solution and refluxed for four hours. The solution was then cooled to room temperature and washed four times with water (~50 mL/washing.) The red/purple solution was dried with sodium sulfate and subsequently filtered and concentrated. The shiny purple solid was analyzed by H-NMR in DMSO-d6 and confirmed to be pyridone linked zinc tetraphenylporphine.

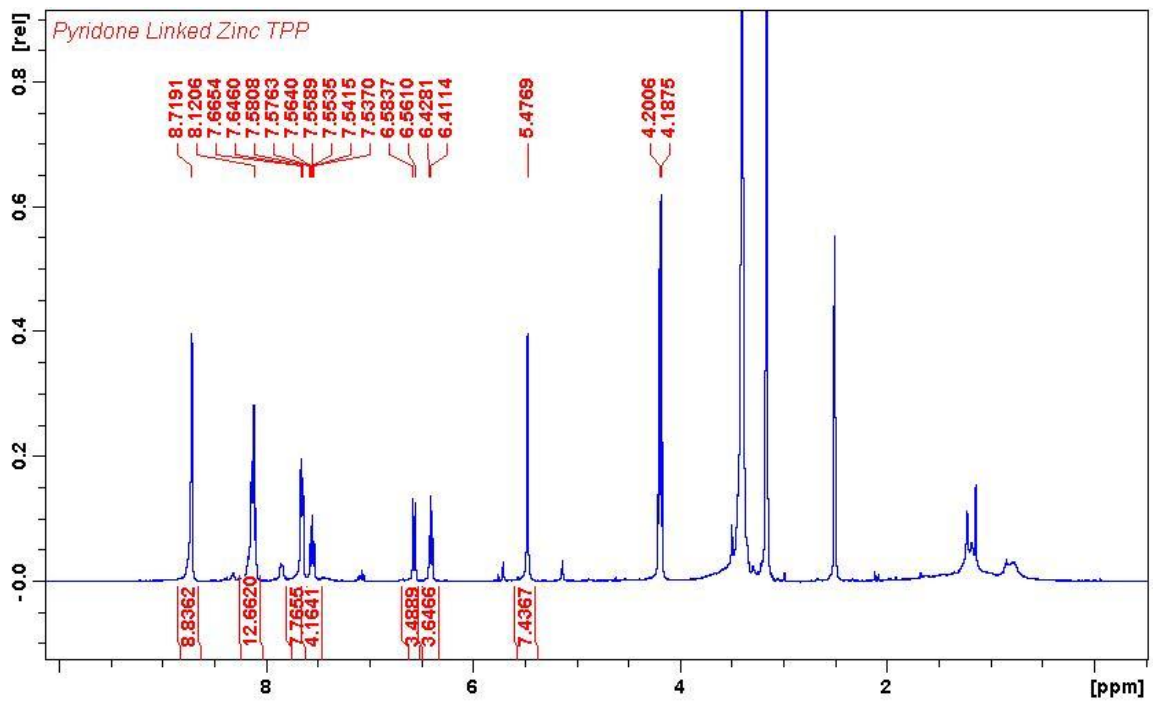

Figure 11 - H NMR Spectrum of Pyridone Linked Zinc Tetraphenylporphine in DMSO-d6

The H NMR spectrum shown in figure 11 is very similar to the free base pyridine linked TPP. However, the two can be distinguished because no 2 proton singlet appears around -2.3 ppm in the zinc porphyrin spectrum, indicating that the two protons have been removed from the inner core of the porphyrin and have been replaced by a Zn^{2+} ion. Additionally, some of the signals experience minor changes in chemical shift. Consequently, at 8.1 ppm, the two signals from one of the phenyl hydrogens and one of the pyridone hydrogens overlap to form what appears to be a 12 proton multiplet. The peaks between 0 ppm and 4.5 ppm are a result of solvent impurities.

Effects of Metallation on Absorbance Properties

Fundamental to understanding the effects of coordinating a zinc ion to the center of the porphyrin ring on singlet oxygen production, is an analysis of the UV/Vis spectra.

Solutions of both the free base pyridone linked TPP and the pyridone linked ZnTPP were prepared in dichloromethane and scanned on a UV/Vis spectrometer. Because the porphyrin Sorret band is such an intense absorption, the amounts of material used were very small and could not be precisely measured. As a result, the exact concentrations of each solution are unknown.

Irradiation of Pyridone Linked Porphyrins

A simple H-NMR experiment is a quick way to qualitatively demonstrate both of the pyridone linked porphyrins' ability to reversibly store singlet oxygen. Choosing the right solvents for this experiment was essential. It was important to have a deuterated solvent in which singlet oxygen had a relatively long lifetime. Deuterated chloroform was one such solvent. Because the free base pyridone linked porphyrin was adequately soluble in chloroform-d, it was tested first to demonstrate the reversible formation of an endoperoxide. A saturated solution of freebase pyridone linked porphyrin was made using $CDCl_3$ NMR Solvent. The solution underwent a series of H-NMR scans in between cycles of irradiation and heating.

An initial scan of the pyridone linked TPP was recorded, then the sample was irradiated by a xenon lamp with a yellow filter whilst oxygen was gently bubbled up through the solution for 20 minutes. After irradiation, another H-NMR scan of the sample was recorded. The sample was then dipped into a thermal control bath set to 50˚C for 30min. Subsequently the H-NMR spectrum was recorded. A total of 3 cycles with varying irradiation and heating repetitions were conducted. Table 1 provides the details of each cycle.

Table 1 - Irradiation and Heating Cycles of Free Base Pyridone Linked TPP

Cycle 1	Irradiation	20 min
	Heating	30 min
Cycle 2	Irradiation	20 min
	Heating	60 min
Cycle 3	Irradiation	60 min
	Heating	60 min

The pyridone linked ZnTPP was not sufficiently soluble in chloroform-d. As a result, the experiment was carried out using dimethylformamide-d7 as the NMR solvent. The experiment was carried out in the same manner as the free base pyridone linked TPP experiment but with slightly different cycle times. Table 2 provides the details of each cycle.

Table 2 - Irradiation and Heating Cycles of Pyridone Linked Zinc TPP

Cycle 1	Irradiation	20 min
	Heating	30 min
Cycle 2	Irradiation	20 min
	Heating	30 min
Cycle 3	Irradiation	30 min
	Heating	60 min

Results

UV/Vis absorbance properties

Coordinating a zinc ion to the center of the pyridone linked TPP resulted in major changes to the UV/Vis spectrum.

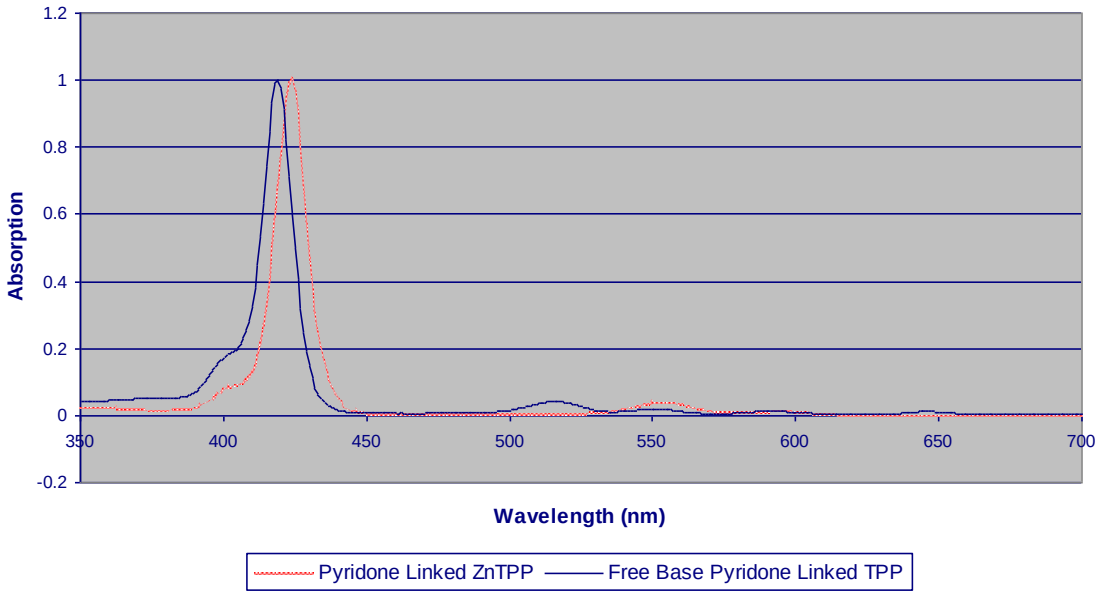

Figure 12 - UV/VIS Spectra of Metallated and Free Base Pyridone Linked Porphyrins

Shown in figure 12 are the UV/VIS spectra of metallated and free base pyridone linked TPP. The Soret band shifted from 419 nm to 424 nm as a result of coordination with a zinc ion. The Q band underwent major changes as a result of metallation. The most notable difference between the two spectra is the fact that the freebase porphyrin has 4 peaks (415 nm, 551 nm, 591 nm, 645 nm) in the Q band and the metalloporphyin only has 2 peaks (554 nm, 596 nm).

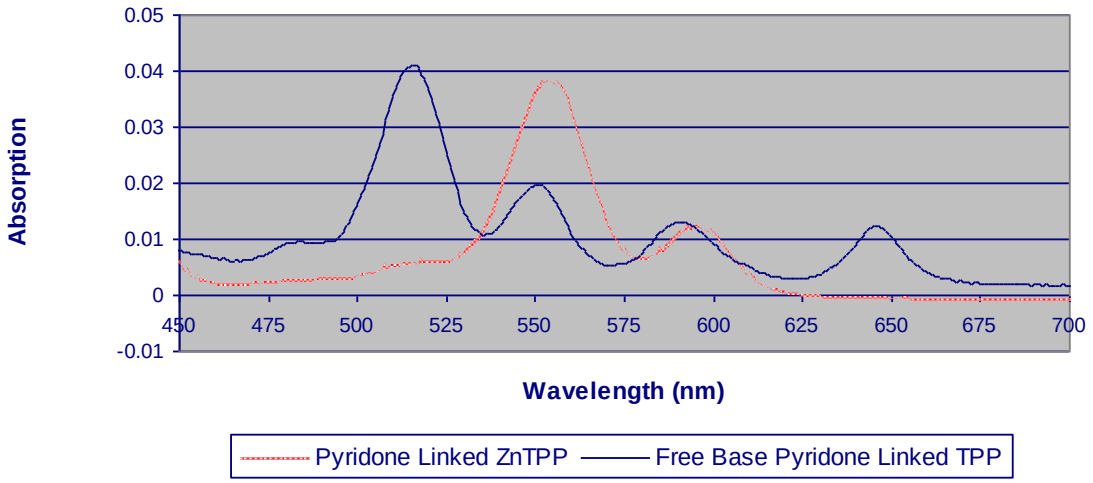

Figure 13 - UV/VIS Spectra of Metallated and Free Base Pyridone Linked Porphyrins Expanded in Q Band Region

Reversible Endoperoxide Formation

The H-NMR experiment conducted on the freebase pyridone linked TPP clearly demonstrated the reversible formation of an endoperoxide. Figure 8 shows the H-NMR spectra taken after each irradiation and heating. It is clearly shown that peaks corresponding to 1,4-endoperoxides on the 2-pyridone grow as a result of irradiation and diminish as a result of heating.

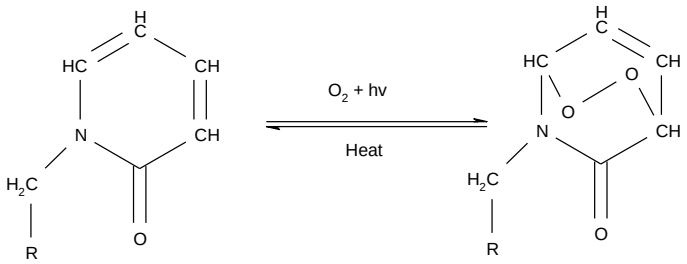

Figure 14 - Endoperoxide Formation Reaction

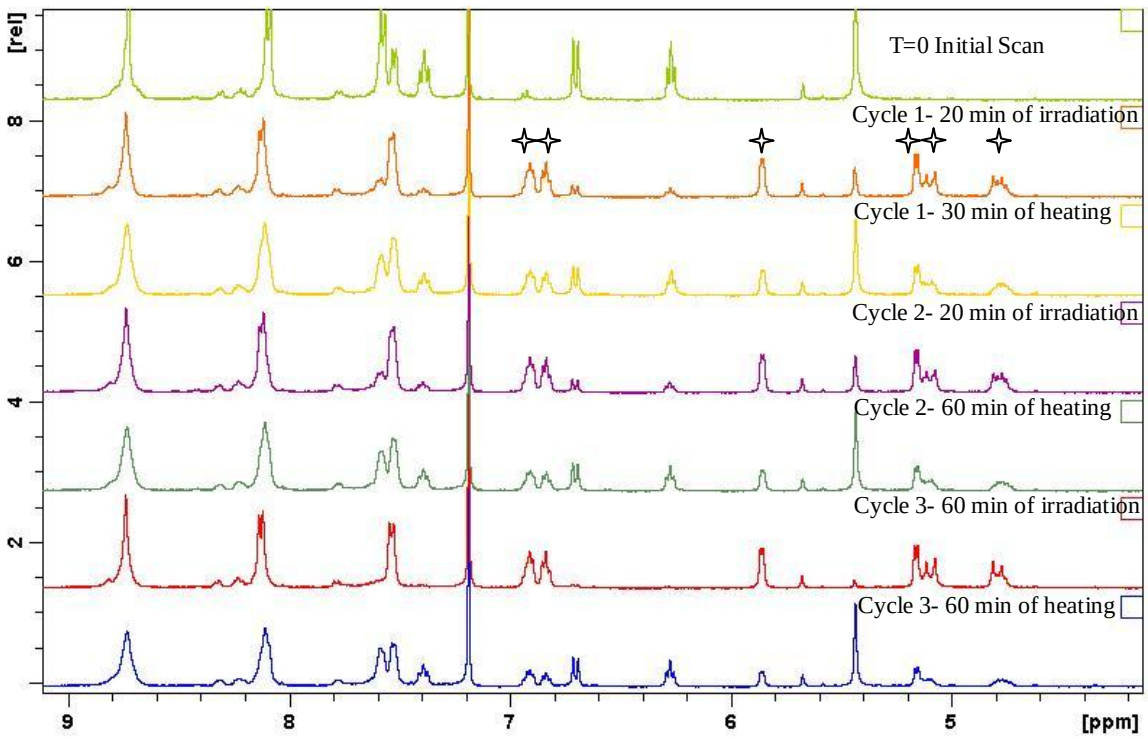

Figure 15 - Overlay of H-NMR Spectra in $CDCl_3$ from Free Base Pyridone Linked TPP Irradiation Experiment

Shown in figure 15 is the overlay of proton NMR spectra from the free base pyridone linked TPP irradiation experiment. When singlet oxygen reacted with free base pyridone linked TPP, 5 signals in the H-NMR spectrum diminished and 6 new signals (starred in second spectrum from top) arose. In the endoperoxide, the methylene protons, which reside in the Pyridone-Porphyrin link, generated two doublets at 4.8ppm and 5.1 ppm. In the normal pyridone linked porphyrin, these two protons were represented by a singlet at 5.4 ppm, a signal which diminished upon irradiation. The four pyridone proton signals at 7.5 ppm, 7.4 ppm, 6.7 ppm, and 6.3 ppm were shifted to 6.9 ppm, 6.8 ppm, 5.9, and 5.2 ppm. The general trend of this shift was to lower chemical shifts as a result of decreased conjugation in the endoperoxide. The results of this experiment demonstrate

the ability of free base 2-pyridone linked TPP to reversibly store singlet oxygen repeatedly without being decomposed.

Reversible formation of the endoperoxide was also clearly demonstrated with the pyridone linked ZnTPP. The spectrum of the metalloporphyrin had different chemical shifts than the free base porphyrin because of the change in solvent. Because of shimming problems on the NMR spectrometer, the signals of interest arose between 0-4 ppm instead of 4-9 ppm. Nevertheless, formation and decomposition of the endoperoxide occurred and is demonstrated by the following set of spectra.

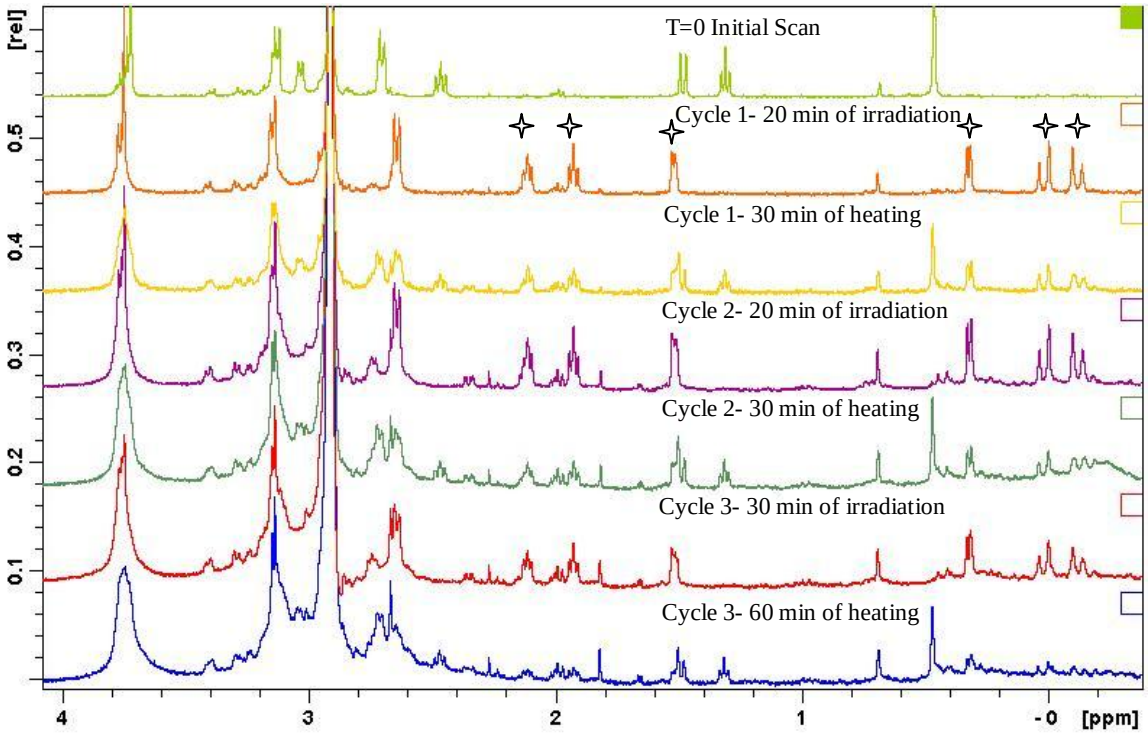

Figure 16 - Overlay of H-NMR Spectra in DMF-d7 from Pyridone Linked ZnTPP Irradiation Experiment

Shown in figure 16 is the overlay of proton nmr spectra from the pyridone linked ZnTPP experiment. As with the free base porphyrin, 6 new signals (stared in second spectrum from top) arose as a result of the endoperoxide formation. The methylene protons gave rise to 2 doublets at -0.1 ppm and 0.0 ppm. The four pyridone protons gave rise to signals at 0.3 ppm, 1.5 ppm, 1.9 ppm, and 2.1 ppm. These 6 peaks rose after irradiations and diminished after heating. After irradiations, the peaks which correspond to the 2-pyidone were completely removed from the spectra. This suggested that endoperoxide formation occurred to completion after only 20 minutes of irradiation. For the free base pyridone linked TPP, only after 60 minutes of irradiation did the 2-pyridone appear to be completely converted to endoperoxide.

Discussion

As a result of this research, a novel porphyrin has been synthesized. The total synthesis of pyridone linked zinc tetraphenylporphine was very challenging, but after the extensive work and the detailed documentation of each step of the synthesis, it should be easily repeated and the final product should be generated quickly and efficiently. Although the synthetic method described in this report is suitable, there still may be room for improvement. Further research should be conducted into each step of the synthesis in order to maximize the yield.

It may be possible to couple the last two reactions, 2-pyridone linkage and metallation, carrying them out as two steps in one pot. The reaction conditions for the two steps are very similar; they simply involve refluxing reactants for several hours. First, tetrakis(a-bromo-p-tolyl)porphyrin should be refluxed with 2-pyridone in THF. Subesquently, zinc acetate in methanol should be added to the refluxing solution. Given enough time for each step to run to completion, the final product should be the pyridone linked zinc TPP. If this is possible, the time required to perform the total synthesis would be reduced dramatically.

It has been clearly demonstrated that both the free base pyridone linked TPP as well as the pyridone linked ZnTPP can reversibly store singlet oxygen in the form of an endoperoxide. The H-NMR studies conducted on these two compounds also suggest that the metallated porphyrin generates the endoperoxide faster than the free base porphyrin. However, because the two studies were done in different solvents and the exact concentrations of the NMR solutions were unknown, it is impossible to definitively conclude which porphyrin is superior. Further examination into this question should be

conducted. Research should also be conducted to determine if endoperoxide formation can be driven by irradiation from the sun.

Pyridone linked porphyrins show a great deal of promise as reversible singlet oxygen sensitizing and storing molecules. The next task is to determine how pyridone linked porphyrins will perform as self-detoxifying materials. Masakatsu Matsumoto[5] has demonstrated the ability of endoperoxides formed from N-substituted 2-pyridones to oxidize tetramethylethylene. 2-Pyridone linked porphyrins should be tested to see if they can demonstrate the same oxidizing power. If successful, the porphyrins should be subsequently tested with chemical warfare agent simulants such as 2-chloroethyl ethyl sulfide and biological agents.

Singlet oxygen trapping porphyrins fit the criteria for an ideal self-detoxifying material. They are self-regenerating as demonstrated by this study and should show strong reactivity with a great number of chemical warfare agents. Singlet oxygen is a high energy and highly reactive species. What makes a singlet oxygen trapping porphyrin system particularly exciting is its versatility. This research along with our general understanding of porphyrins and singlet oxygen suggests that a fabric system containing a singlet oxygen trapping porphyrin component would provide protection simply from being in direct sunlight in an oxygen rich environment. Furthermore, because the porphyrin component can store singlet oxygen, that protection would be extended into periods of darkness. Research thus far has indicated that the desired properties for a self-detoxifying material can be provided by pyridone linked porphyrins.

References

[1] Block, S. M. *American Scientist* 2001, *89*, 28.
[2] Smith, B. M. *Chem. Soc. Rev.*, 2008, 37, 470 - 478
[3] Changtong, C.; Shuster, C.; Lombardi, J. L.; Connors, R. E. *Composite Molecules that Generate, Store, and Release Singlet Oxygen.* 34th Northeast Meeting of the American Chemical Society, Binghampton, N.Y., Oct. 2006.
[4] DeRosa, M. C.; Crutchley, R. J. *Coordination Chemistry Reviews* 2002, *233-234*, 351-371.
[5] Matsumoto, M.; Yamada, M.; Watanabe, N. *Chemical Communications* 2005, 483-485.
[6] Turro, N. J. In *Singlet Oxygen and Chemiluminescent Organic Reactions;* Modern Molecular Photochemistry; University Science Books: Sausalito, Ca, 1991; pp 579.
[7] Milgrom, L. R. In *The Colours of Life: An Introduction to the Chemistry of Porphyrins and Related Compounds;* Oxford University Press: Oxford, UK, 1997.
[8] Rothemund, P. *J. Am. Chem. Soc.* 1935, *57*, 2010-2011.
[9] Rothemund, P. *J. Am. Chem. Soc.* 1936, *58*, 625-627.
[10] Lindsey, J. S.; Schreiman, I. C.; Hsu, H. C.; Kearney, P. C.; Marguerettaz, A. M. *J. Org. Chem.* 1987, *52*, 827-836.
[11] Foote, C. S.; Clennan, E. L. In *Properties and Reactions of Singlet Dioxygen;* Active Oxygen in Chemistry; 1995; pp 105-140.